Pressure-induced change of the stereochemical activity of a lone electron pair

Björn Winkler
Mineralogisch-Petrographisches Institut der Christian Albrechts Universität, Olshausenstrasse 40, D-24098 Kiel, Germany

Victor Milman
MSI, 240/250 The Quorum, Barnwell Road, Cambridge CB5 8RE, United Kingdom

Ming-Hsien Lee
Department of Physics, Tamkang University, Tamsui, Taipei 251, Taiwan

(Received 8 September 1997; accepted 30 December 1997)

Ab initio total energy calculations based on density functional theory and the generalized gradient approximation in conjunction with a constant pressure minimization algorithm have been used to demonstrate that the pressure-induced phase transition from a rhombohedrally distorted into an ideal cubic structure of $CsGeCl_3$ involves a change in the stereochemical activity of the lone electron pair from ''active'' to ''inert.'' © *1998 American Institute of Physics.* [S0021-9606(98)02413-1]

INTRODUCTION

The structure of $CsGeCl_3$ at ambient pressure may be described as a rhombohedrally distorted perovskite (Fig. 1).[1] A peculiarity of the $CsGeCl_3$ structure at ambient conditions is the $3+3$ coordination of the Ge atom, where three Ge–Cl bonds are 2.35 Å long, while the three other Ge–Cl distances in the very distorted octahedra are longer than 3.0 Å, and hence are often considered as ''nonbonding''. This atomic arrangement is thought to be due to the stereochemical activity of the lone electron pair of the Ge atom, which, within the standard ''valence shell electron pair repulsion'' (VSEPR) model,[2] will lead to observed Cl–Ge–Cl angles of $\approx 90°$. Above 2.7 GPa the structure of $CsGeCl_3$ is cubic with space group $Pm3m$.[3] The phase transition into the undistorted cubic perovskite structure involves a shortening of the nonbonding distances, which leads to a symmetrization of the coordination polyhedron of the Ge atom into a regular octahedron. It has therefore been suspected that this implies a fundamental change in the ''character'' of the lone electron pair.[3] A stereochemical activity of the $4s^2$ electrons of the Ge atom implies a significant admixture of p character as only then there will be an anisotropic electron density. The point symmetry of the position of the Ge atom in the high pressure phase implies a stereochemically inert lone electron pair with pure s character. Such a change in the electron density cannot currently be determined experimentally, as it would involve measuring minute changes in the electron density under pressure. Here, a theoretical study can provide a confirmation of the intuitive explanation.

Density functional calculations[4,5] are currently the most widely used theoretical approaches for the simulation of properties of condensed matter. Due to recent progress for the approximation of the exchange–correlation potential leading to the generalized gradient approximation (GGA),[6] the often encountered overbinding due to the local density approximation has generally been overcome. A further recent achievement is the development of constant pressure minimization algorithms which allow the relaxation of low symmetry structures at a prescribed external pressure.[7]

COMPUTATIONAL DETAILS

Commercial (MSI) and academic versions of the software package CASTEP (Cambridge Serial Total Energy Package), which has been described elsewhere,[8,9] and associated programs for symmetry analysis were used for the calculations presented here. CASTEP is a pseudopotential total energy code which employs special points integration over the Brillouin zone, and a plane-wave basis set for the expansion of the wave functions. The calculations were performed using norm-conserving nonlocal pseudopotentials of the form suggested by Kleinman and Bylander,[10] where the pseudopotentials were taken from the CASTEP database. We used two different pseudopotentials for Ge in the calculations. In one Ge pseudopotential, the $3d$ electrons were included into the frozen core and only the $4s$ and $4p$ electrons were treated as valence electrons. In the other pseudopotential, the $3d$ electrons were treated as valence electrons as well. A gradient-corrected form of the exchange–correlation functional (GGA) was used in the form suggested by White and Bird.[11] A cutoff of 900–1200 eV for the kinetic energy for the plane wave expansion of the wave functions was chosen to ensure numerical stability of the constant pressure minimizer. This corresponds to more than 15 000 plane waves at each of the six k points determined according to Monkhorst and Pack[12] in the irreducible wedge of the Brillouin zone. Initially, the calculations were started with a rhombohedral lattice with space group $R3$, but as the relaxed structures all had higher symmetry (namely, at least $R3m$, see below) some of the calculations were then started with $R3m$ symmetry. This did not change the results, but improved the convergence behavior. Geometry optimization was performed using the BFGS minimization technique.[7] In this scheme the Hessian matrix in the mixed space of internal

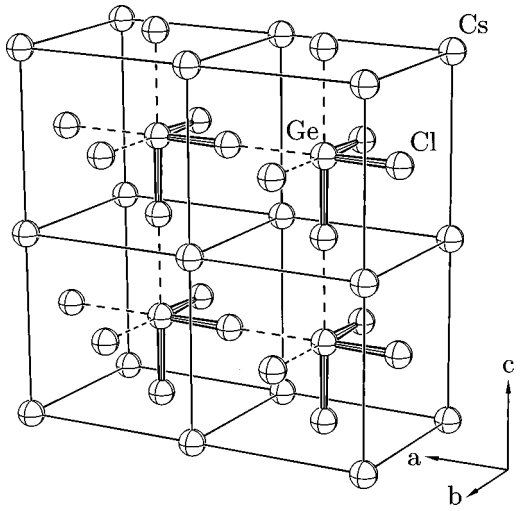

FIG. 1. The structure of $CsGeCl_3$ at ambient pressure. The Ge–Cl bonds are indicated, while the long, nonbinding Ge–Cl– distances are shown as single dashed lines.

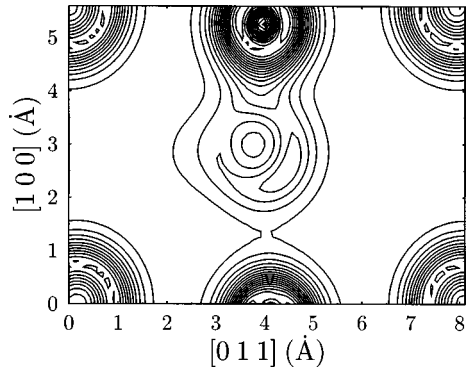

FIG. 2. Contour plot of the calculated valence electron density along a (110) section in $CsGeCl_3$ at ambient pressure. The interval between adjacent contour lines is $0.1\,e/Å^3$. There is a clear anisotropy of the electron density close to the Ge atom, which is located at the center of the figure, corresponding to the lone electron pair. The distance from the local maximum in the electron density to the Ge atom is about 0.75 Å. Also shown is the covalent bonding to the Cl atom located close to the middle of the upper border, while there is no significant bonding to the Cl atom close to the middle of the lower border.

coordinates and cell variables is updated using *ab initio* calculated atomic forces and the stress tensor and taking into account symmetry-related constraints. Pulay stress correction was evaluated numerically by performing total energy calculations at three different values of the kinetic energy cutoff.[13] Calculations were considered converged when the residual forces on the atoms were less than 0.025 eV/Å, the displacements of atoms during the geometry optimization steps were less than 0.001 Å, and the residual bulk stress was less than 0.05 GPa. For soft molecular compounds, these are strict convergence criteria.

RESULTS

The structural parameters of the calculated structure at 0 GPa are given in Table I. Independent of the pseudopotential used for the Ge, the lattice parameters for the low pressure phase are in good agreement with experiment. From the predicted bond length, however, it is obvious that the inclusion or neglect of the Ge-3*d* electrons leads to significant changes in the description of the inter- and intramolecular bonds. If the 3*d* electrons are not treated as valence electrons, the covalent Ge–Cl bond is too short by 3.2%, while the nonbonded Ge–Cl′ distance is too long by 4.3%. However, if the Ge 3*d* electrons are treated as valence electrons, then the Ge–Cl bond length is too large by 2.7% while the nonbonded distance is too short by 1.8%. In the latter case, the bond angles within the $GeCl_3$ group are in better agreement with experimental data. Hence, by treating the 3*d* electrons of Ge as valence electrons, the pseudoatom becomes slightly ''bigger,'' which pushes the covalently bonded Cl further away, while at the same time decreasing the nonbonding distance. A similar problem was discussed in GaN, where the 3*d* electrons for Ga had to be treated as valence electrons.[14] However, for the question addressed here, this different behavior and the discrepancy between experiment and theory is irrelevant, as we will show that in both cases the pressure-induced change in the electron density distribution is the same.

TABLE I. Experimentally determined (Ref. 1) and calculated structural parameters of $CsGeCl_3$ at 0 GPa. The Cs atom is located at 0,0,0, the Ge atom at *x*,*x*,*x*, and the Cl atom at *x*,*x*,*z*. Calculations were performed with the 3*d* electrons included in the frozen core (1) or treated as valence electrons (2).

		Expt.	Calc. (1)	Diff. (%)	Calc. (2)	Diff. (%)
Temp.	(K)	293	···			
a_0		5.434(2)	5.464	+0.6	5.436	0.03
α		89.72(3)	88.77	−1.1	89.03	−0.7
Ge	*x*	0.4854(1)	0.4722		0.4874	
Cl	*x*	0.5024(3)	0.4975		0.5095	
	z	0.0538(3)	0.0583		0.0442	
Ge–Cl	(Å)	2.348(2)	2.272	−3.2	2.412	2.7
Ge–Cl′	(Å)	3.092(2)	3.225	+4.3	3.036	−1.8
Cl–Ge–Cl	(°)	94.16(6)	95.7	+1.6	94.70	0.6
Cl–Ge–Cl′	(°)	89.66(5)	90.0	+0.4	90.25	0.7
Cl′–Ge–Cl′	(°)	86.23(5)	83.7	−3.0	84.30	−2.2

The ambient pressure calculations have all been started assuming space group $R3$, but the relaxed structure had space group $R3m$. This confirms the results of a recent study,[1] which concluded that the space group $R3$ found in an earlier study for the ambient pressure phase[15] was erroneous. A contour plot of the calculated valence electron charge density of the 0 GPa structure for a (110) section is displayed in Fig. 2. This result was obtained with the Ge 3*d* electrons treated as part of the frozen core. In Fig. 2 and the following figures, the origin of the lattice is taken to be at the Cs atom. Figure 2 clearly shows the anisotropy of the charge density around the Ge atom. There are two reasons for this anisotropy, namely, the covalent bond to the ''near'' Cl atoms and a stereochemically active lone electron pair. This becomes more evident from Fig. 3, where the difference between the superposed electron densities of free atoms placed on their lattice sites and the self-consistent electron density of the crystal is shown. In the calculation shown only the valence electrons have been used explicitly (nine for Cs, seven for Cl, and four for Ge). The ''lone electron pair'' close to the Ge atom is much easier to observe when only the four out-

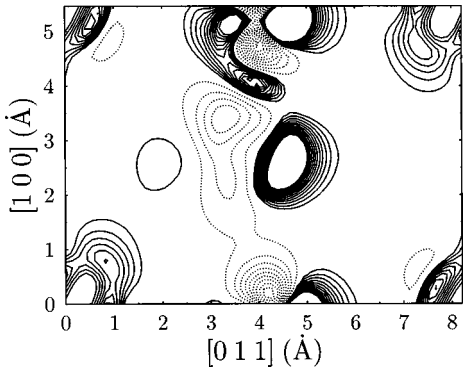

FIG. 3. Contour plot of a (110) section of the difference between the self-consistent valence charge density in the crystal and a superposition of the atomic charge densities. The atomic positions are the same as in Fig. 2. Dashed lines indicate that the charge density in the crystal is less than the charge density obtained from the superposed atomic charge densities. Full lines mark the regions where the charge density in the crystal is larger than the superposition of the atomic charge densities. The distance between adjacent dashed contour lines is $0.025\ e/\text{Å}^3$, that between full lines is $0.005\ e/\text{Å}^3$. The maximum close to the center of the figure corresponds to the lone electron pair.

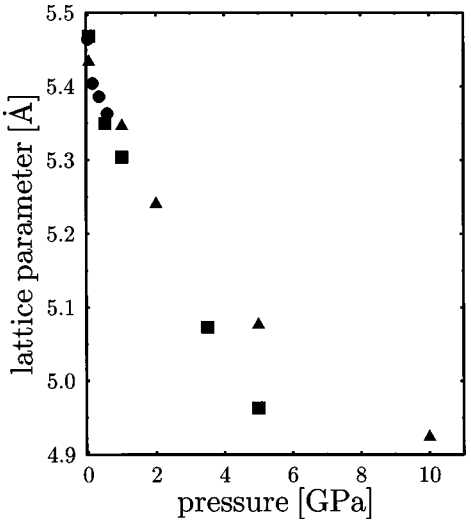

FIG. 4. Comparison of experimentally determined (Ref. 18) values, shown as dots, and the calculated data of the lattice constants. The squares represent results from calculations where the Ge $3d$ electrons were included in the pseudopotential, while the triangles represent values from those calculations where the Ge $3d$ electrons were treated as valence electrons.

ermost electrons are used in the calculations, but is unchanged when the second pseudopotential with fourteen valence electrons for Ge is used. The local maximum of the electron density in the crystal corresponding to the lone electron pair is about 0.7 Å away from the Ge atom. The local maximum in the electron density which is approximately halfway between the near Cl atom and the Ge atom is due to the covalent bonding between these two atoms. Calculations such as those performed here do not allow one to determine the charge of the lone electron pair unambiguously, as the integration boundaries would have to be chosen arbitrarily. Also, for a comparison to the valence electron of the high pressure phase, this was not necessary.

On increasing pressure, there is a continuous change in the structural parameters, as shown in Figs. 4 and 5. The corresponding pressure dependence of the cell volume is given in Fig. 6, where a simple Birch equation of state[16]

$$V = V_0 \left(1 + \frac{B'}{B_0} P \right)^{-1/B_0}$$

has been fitted to the data, where B' is the pressure derivative of B_0,

$$B' = \frac{\partial B_0}{\partial P}.$$

The calculated bulk modulus for the calculations without Ge $3d$ valence electrons gives $V_0 = 163.6\ \text{Å}^3$, $B_{0,\text{I}} = 7.9$ GPa, and a pressure derivative, $B'_{\text{I}} = 4.8$, while the calculations with Ge $3d$ electrons gave $V_0 = 161.4\ \text{Å}^3$, $B_{0,\text{II}} = 13.67$ GPa, and $B'_{\text{II}} = 5.1$.

The elastic properties calculated are reasonably similar to those given by Ref. 17 for Cs-halides, which have $B_0 \approx 12-17$ GPa, and $B' = 6$. The discrepancy with the data given for $CsGeCl_3$ by Knorr *et al.*,[18] who derived a bulk modulus of $B_0 = 1.5$ GPa and a $B' = 55$, is most probably due to the experimental difficulties encountered in the high pressure neutron diffraction experiments, which make an inter- and extrapolation between the few data points obtained in that study unreliable.

With increasing pressure, the rhombohedral angle tends toward 90° and the Cl position moves to the center of the faces of the cube. The current calculations could not be used to investigated the disordered intermediate phase between the ambient pressure structure and the high pressure structure.[3] From spectroscopic experiments, the transition into the ordered high pressure phase occurs at 2.7 GPa.[3] The current calculations show that within the limits of accuracy

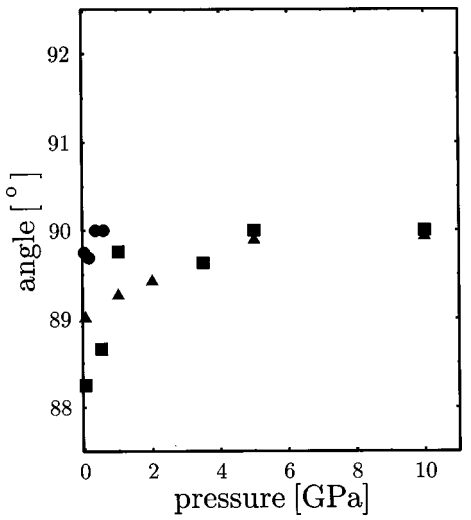

FIG. 5. Comparison of experimentally determined (Ref. 18) values, shown as dots, and the calculated data for the rhombohedral angle. The squares represent results from calculations where the Ge $3d$ electrons were included in the pseudopotential, while the triangles represent values from those calculations where the Ge $3d$ electrons were treated as valence electrons. Within the accuracy of the calculations, the structure is cubic above 5 GPa, irrespective of the pseudopotential used. This is also evident from the atomic positions, which correspond to a cubic perovskite structure above this pressure.

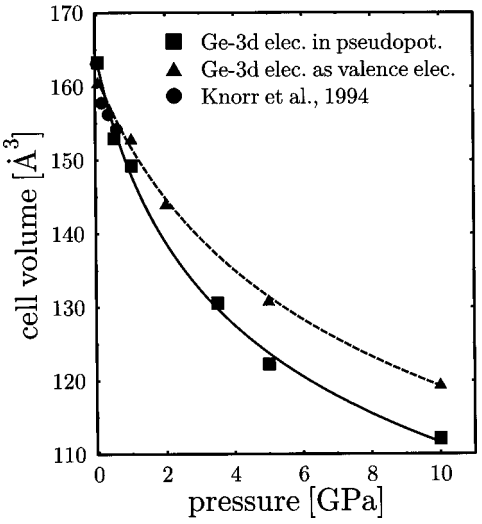

FIG. 6. Calculated and observed (Ref. 18) pressure dependence of the unit-cell volume of $CsGeCl_3$. The fits of an equation-of-state to the calculated values are given by the lines, the corresponding parameters are given in the text.

the symmetry of the $CsGeCl_3$ structure above 5 GPa is cubic. This upper limit for the transition pressure is thought to be in good enough agreement with experimental data, and hence the analysis of the electron density at high pressure was based on this calculation.

A projection of the calculated electron density similar to that shown before for the 0 GPa structure in Fig. 2 is shown for the 5 GPa structure in Fig. 7. A comparison of these two figures indicates the fundamental change of the symmetry of the electron density around the Ge atom. The cubic symmetry observed in the calculations for the high pressure phase excludes an anisotropy of the electron density such as had been observed in the calculations for the low pressure structure, and this implies that the stereochemical activity of the lone electron pair at the Ge atom is lost when pressure is applied to the system.

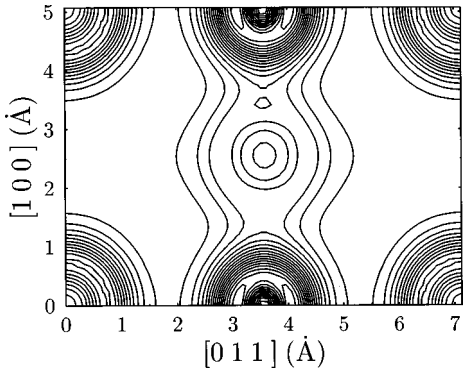

FIG. 7. Contour plot of the electron density on (011) at 5 GPa. The Ge atom, located at $\frac{1}{2}\frac{1}{2}\frac{1}{2}$ is now in a regular sixfold coordination and there is no local maximum of the electron density close to it. Small deviations from cubic symmetry of the electron density are due to numerical inaccuracies, as the calculations were performed without constraining the symmetry of the density or the potential to be cubic. A comparison to Fig. 2 clearly shows that there is no stereochemically active lone electron pair close to the Ge atom at 5 GPa.

DISCUSSION

The current calculations have shown the applicability of the VSEPR model for the explanation of the formation of the pseudotrigonal coordination of Ge atoms in the low pressure phase. They have also demonstrated that the pressure-induced change of the electron density distribution leads to a symmetrization of the electron density around the Ge atom and hence allows the formation of an undistorted perovskite structure. The experimental difficulties associated with the determination of small changes in the electron density have prevented detailed studies of electron density distributions at high pressures. Hence, a model such as VSEPR theory can only be tested by computer simulation, and the current study has unambiguously demonstrated that state-of-the-art density functional theory calculations in conjunction with a constant pressure relaxation algorithm can provide insights with respect to subtle changes in the electron density distribution not obtainable experimentally.

ACKNOWLEDGMENTS

We would like to thank F. Liebau (Kiel) for a critical reading of an earlier version of the manuscript. We are grateful to Carsten Griewatsch (Kiel) for the ORTEP plot of the $CsGeCl_3$ structure. B.W. is grateful for financial support form the Deutsche Forschungsgemeinschaft through Grant No. Wi-1232/1-1.

[1] G. Thiele, H. W. Rotter, and K. D. Schmidt, Z. Anorg. Allg. Chem. **545**, 148 (1987).
[2] R. J. Gillespie, J. Chem. Educ. **40**, 295 (1963).
[3] H. Hillebrecht, U. Schwarz, K. Syassen, H. G. von Schnering, and G. Thiele, Proceedings of the ECM-15, 1994 (unpublished), p. 615.
[4] R. O. Jones and O. Gunnarsson, Rev. Mod. Phys. **61**, 689 (1989).
[5] R. G. Parr and W. Yang, *Density-Functional Theory of Atoms and Molecules* (Oxford University Press, Oxford, 1989).
[6] J. P. Perdew and Y. Wang, Phys. Rev. B **45**, 13244 (1992).
[7] T. H. Fischer and J. Almlöf, J. Phys. Chem. **96**, 9768 (1992).
[8] M. P. Teter, M. C. Payne, and D. C. Allan, Phys. Rev. B **40**, 12255 (1989).
[9] M. C. Payne, M. P. Teter, D. C. Allan, T. A. Arias, and J. D. Johannopoulos, Rev. Mod. Phys. **64**, 1045 (1992).
[10] L. Kleinman and D. M. Bylander, Phys. Rev. Lett. **48**, 1425 (1982).
[11] J. A. White and D. M. Bird, Phys. Rev. B **50**, 4954 (1994).
[12] H. J. Monkhorst and J. D. Pack, Phys. Rev. B **13**, 5188 (1976).
[13] G. P. Francis and M. C. Payne, J. Phys.: Condens. Matter **2**, 4395 (1990).
[14] M. Palummo, L. Reining, R. W. Godby, C. M. Bertoni, and N. Bornsen, Europhys. Lett. **26**, 607 (1994).
[15] A. N. Christensen and S. E. Rasmussen, Acta Chem. Scand. **19**, 421 (1965).
[16] R. L. Hazen and L. W. Finger, *Comparative Crystal Chemistry* (Wiley, New York, 1982).
[17] U. Köhler, P. G. Johannsen, and W. B. Holzapfel, J. Phys.: Condens. Matter **9**, 5581 (1997).
[18] K. Knorr, W. Depmeier, and I. Kaiser, BENSC Experimental Reports, 1994, pp. 223, 224.